BIOCHEMISTRY
including biophysical chemistry & molecular biology

Article

pubs.acs.org/biochemistry

Effects of Tau Domain-Specific Antibodies and Intravenous Immunoglobulin on Tau Aggregation and Aggregate Degradation

Jose O. Esteves-Villanueva,[†] Hanna Trzeciakiewicz,[†] David A. Loeffler,[‡] and Sanela Martić*[,†]

[†]Department of Chemistry, Oakland University, 2200 North Squirrel Road, Rochester, Michigan 48309, United States

[‡]Department of Neurology, Beaumont Health System, 3811 West Thirteen Mile Road, Suite 507, Royal Oak, Michigan 48073, United States

Supporting Information

ABSTRACT: Tau pathology, including neurofibrillary tangles, develops in Alzheimer's disease (AD). The aggregation and hyperphosphorylation of tau are potential therapeutic targets for AD. Administration of anti-tau antibodies reduces tau pathology in transgenic "tauopathy" mice; however, the optimal tau epitopes and conformations to target are unclear. Also unknown is whether intravenous immunoglobulin (IVIG) products, currently being evaluated in AD trials, exert effects on pathological tau. This study examined the effects of anti-tau antibodies targeting different tau epitopes and the IVIG Gammagard on tau aggregation and preformed tau aggregates. Tau aggregation was assessed by transmission electron microscopy and fluorescence spectroscopy, and the binding affinity of the anti-tau antibodies for tau was evaluated by enzyme-linked immunosorbent assays. Antibodies used were anti-tau 1−150 ("D-8"), anti-tau 259−266 ("Paired-262"), anti-tau 341−360 ("A-10"), and anti-tau 404−441 ("Tau-46"), which bind to tau's N-terminus, microtubule binding domain (MBD) repeat sequences R1 and R4, and the C-terminus, respectively. The antibodies Paired-262 and A-10, but not D-8 and Tau-46, reduced tau fibrillization and degraded preformed tau aggregates, whereas the IVIG reduced tau aggregation but did not alter preformed aggregates. The binding affinities of the antibodies for the epitope for which they were specific did not appear to be related to their effects on tau aggregation. These results confirm that antibody binding to tau's MBD repeat sequences may inhibit tau aggregation and indicate that such antibodies may also degrade preformed tau aggregates. In the presence of anti-tau antibodies, the resulting tau morphologies were antigen-dependent. The results also suggested the possibility of different pathways regulating antibody-mediated inhibition of tau aggregation and antibody-mediated degradation of preformed tau aggregates.

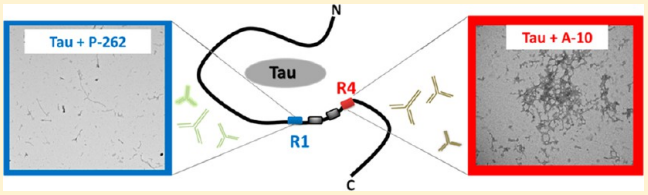

Tau is a microtubule-associated protein found primarily in neurons whose normal functions include microtubule stabilization and regulation of axonal transport.[1] In the human central nervous system (CNS), tau is present as six alternatively spliced isoforms coded within a single gene on chromosome 17. In Alzheimer's disease (AD) and other tauopathies, tau undergoes hyperphosphorylation and aggregation, leading to a variety of tau conformations, including soluble oligomers, neurofibrillary tangles (NFTs), and paired-helical filaments (PHFs). Tau is also found in AD neurophil threads and dystrophic neurites. The significance of NFTs in AD is unclear. Soluble tau oligomers, a species that is intermediate between normally phosphorylated protein tau and hyperphosphorylated tau fibrils, may be the most neurotoxic tau conformation,[2,3] paralleling current thinking regarding Aβ soluble oligomers relative to fibrillar Aβ oligomers.[4] Tau pathology appears to be capable of spreading between cells in the CNS.[5,6] Treatments targeting Aβ have thus far failed to slow AD's clinical progression;[7−9] therefore, tau pathology is attracting increased interest as an AD therapeutic target. In transgenic "tauopathy" mice, the administration of phosphorylated tau[10−15] or monoclonal antibodies to phosphorylated tau[16−18] was found to reduce tau pathology. Treatment of the 3xTg mouse model of AD with an intravenous immunoglobulin (IVIG) that contains specific anti-tau antibodies resulted in a small but statistically significant decrease in hippocampal NFTs (~15%) but no reduction in tau pathology.[19] Further, a tau aggregation inhibitor produced encouraging results in a phase II trial, and its second-generation counterpart is being tested in phase III trials. The reduced tau pathology in the mouse studies cited above could be due to antibody-facilitated phagocytosis of pathological tau[12] and/or antibody-mediated degradation of tau within neurons[20] or possibly even in the neurophil. Anti-tau antibodies may also reduce tau pathology by preventing and/or degrading tau aggregates or preventing their spread in the brain. Human tau isoforms contain either three or four microtubule binding domain (MBD) repeat sequences that consist of highly conserved 18 amino acid repeats separated by less conserved 13 or 14 amino acid inter-repeat sequences.[21] Tau's MBD repeats are required for its aggregation into PHFs,[22] which are present in NFTs, neuropil threads, and dystrophic neurites. The four MBD repeats differ with respect to their aggregation rates and

Received: October 10, 2014
Revised: December 28, 2014
Published: December 29, 2014

DOI: 10.1021/bi501272x
Biochemistry 2015, 54, 293−302

minimum concentrations for starting tau filament extension; the possible role of each repeat in tau's aggregation has been discussed by Tomoo et al.[23] Most of the known tau mutations that are present in frontotemporal dementia and parkinsonism linked to chromosome 17 (FTDP-17), an autosomal dominant neurodegenerative disorder, are found within one of the four MBD repeat sequences. These mutations result in alterations to tau's hydrophobicity and charge and induce potential changes in tau's secondary structure.[24] Antibodies targeting tau's first and second MBDs, but not its C-terminus, were found to inhibit tau fibril formation in vitro.[25] Antibodies to non-phosphorylated tau, infused into the lateral ventricle of tauopathy mice, lowered brain concentrations of aggregated as well as hyperphosphorylated and insoluble tau.[26] A tau oligomer-specific monoclonal antibody was found to reduce brain levels of tau oligomers but not phosphorylated NFTs or monomeric tau.[27] Taken together, these results suggest that therapeutic targeting of both nonphosphorylated and phosphorylated conformations of tau may be useful for the treatment of AD and other tauopathies. The mechanisms by which antibodies reduce tau aggregation are unclear, and it is unknown if the ability of an antibody to influence this process is predictive of its effects on preformed tau aggregates. The objective of this study was to explore these issues. The effects of antibodies targeting various regions of tau (N-terminus, MBD repeat sequences R1 and R4, and C-terminus) as well as the effects of the IVIG product Gammagard on tau aggregation and preformed tau aggregates were examined using transmission electron microscopy (TEM) and fluorescence spectroscopy. The binding affinities of the specific antibodies for tau were also determined by an enzyme-linked immunosorbent assay (ELISA). The antibodies targeting specific tau domains showed evidence of aggregation inhibition and degradation of preformed tau aggregates.

MATERIALS AND METHODS

Materials. Tau-441 protein (recombinant human tau-441, 2N4R) was purchased as a lyophilized powder from rPeptide. Anhydrous dibasic sodium phosphate (Na_2HPO_4) was obtained from J. T. Baker. Phosphoric acid, 2-(*N*-5-morpholino)ethanesulfonic acid (MES), 4-(2-hydroxyethyl)-1-piperazineethanesulfonic acid (HEPES), sodium chloride, ethylenediaminetetraacetic acid (EDTA), dithiothreitol (DTT), and anhydrous monobasic sodium phosphate (NaH_2PO_4) were purchased from Fisher Scientific. Glutaraldehyde (2%), uranyl acetate (1%), and Formvar carbon film on 200 mesh nickel grids were from Electron Microscopy Sciences. Antibodies used in this study were D-8 (mouse monoclonal anti-tau 1−150 [N-terminus sequence], Santa Cruz Biotechnology, TX, USA), Paired-262 (rabbit polyclonal anti-tau 259−266 [MBD repeat sequence R1], AnaSpec, CA, USA), A-10 (mouse monoclonal anti-tau 341−360 [MBD repeat sequence R4], Santa Cruz Biotechnology), and Tau-46 (mouse monoclonal anti-tau 404−441 [C-terminus sequence], Abcam). The IVIG product Gammagard Liquid [immune globulin intravenous (human), 10%] was from Baxter Healthcare Corporation. Human myeloma protein (human IgG1 κ chain) from The Binding Site served as the negative control for IVIG. The ProteoStat protein aggregation assay was purchased from Enzo Life Sciences. SuperBlock blocking buffer was purchased from Thermo Scientific. Biotinylated monoclonal antibody 6E10 and streptavidin−alkaline phosphatase were purchased from Zymed laboratories (Invitrogen/Life Technologies). Optical density measurements were carried out using a V_{max} kinetic microplate reader (Molecular Devices Corporation).

Tau Aggregation. Tau aggregation was performed in the absence of antibodies with a final tau concentration of 900 μg mL^{-1} in a tau buffer solution consisting of 50 mM MES, pH 6.8, 10 mM NaCl, and 0.5 mM EDTA, to which 0.5 μL of 1× PBS (pH 7.4) solution (instead of antibody, see below) was added. Arachidonic acid in ethanol was added to a final concentration of 30 mg mL^{-1} and 3.75% ethanol. Aggregation was performed at 37 °C for 48 h.

Effects of Anti-Tau Antibodies, the IVIG, and Normal Human IgG1 on Tau Aggregation. Tau was diluted to a final concentration of 900 μg mL^{-1} in a buffer consisting of 50 mM MES (pH 6.8), 100 mM NaCl, and 0.5 mM EDTA (pH 6.8), unless otherwise stated, with 0.5 μL of antibody (A-10, D-8, Paired-262, Tau-46, IVIG Gammagard, and the negative control normal human IgG1 [human myeloma protein]) in the presence of arachidonic acid at a final concentration of 30 mg mL^{-1} (3.75% final ethanol concentration). Final A-10, D-8, Paired-262, and Tau-46 antibody concentrations were all 9.1 μg mL^{-1}, and final IVIG Gammagard and normal human IgG1 concentrations were 45 μg mL^{-1}.

Effects of Anti-Tau Antibodies and the IVIG on Preformed Tau Aggregates. Tau aggregates were generated as described above. Then, 0.5 μL of anti-tau antibodies, IVIG Gammagard, normal human IgG1, or PBS was added, and the incubation was continued for an additional 24 h at 37 °C.

Transmission Electron Microscopy. FEI Morgagni 268 (FEI Company) and JEOL 2200FS (Japan Electron Optics Laboratories) transmission electron microscopes were used. For each experimental condition, two grids were made and examined at 22000× and 56000× magnification. Tau aggregates were diluted in 20 μL of buffer (50 mM MES (pH 6.8), 100 mM NaCl, 0.5 mM EDTA (pH 6.8)). Ten microliters of the diluted sample was placed on a Formvar carbon film on 200 mesh nickel grids for 10 or 60 min. The grid was then blotted with filter paper, rinsed with deionized water, and again blotted with filter paper. One drop of 2% glutaraldehyde was placed on the grid for 10 min and then blotted dry and rinsed with deionized water. One drop of 1% uranyl acetate was placed on the grid for 5 min, blotted, rinsed, and blotted dry. Grids were then imaged via TEM. All TEM studies were performed as two independent experiments (two grids per experiment) for each condition.

Fluorescence Spectroscopy. Fluorescence measurements were carried out on Synergy H1 (Biotek) using Take3 microwell plates (Biotek). Each well contained 3 μL of solution, and four wells were used for a single condition. Each condition was repeated in duplicate (for a total of eight wells per condition). Time-dependent experiments were performed using aggregation times of 0, 3, 5, 8, 10, 15, 30, and 60 min and 2, 3, 4, 6, 8, 12, 24, and 48 h. Concentration-dependent experiments were carried out at tau concentrations of 0, 1, 10, 100, and 1000 pg mL^{-1}, 10, 100, and 1000 ng mL^{-1}, and 10, 100, 200, 300, 400, 500, 600, 700, 800, 900, and 1000 μg mL^{-1}. For the aggregation study, the aggregation mixture was prepared by mixing tau (900 μg mL^{-1}), arachidonic acid (30 mg mL^{-1}), and antibody (9 or 45 μg mL^{-1}). The solution was incubated for 48 h at 37 °C, and then ProteoStat reagent was added prior to the measurement. For the disaggregation study, the aggregates were first formed by mixing tau (900 μg mL^{-1}) and arachidonic acid (30 mg mL^{-1}) and incubating them for 48 h at 37 °C. Subsequently, antibody (9 or 45 μg

DOI: 10.1021/bi501272x
Biochemistry 2015, 54, 293−302

mL^{-1}) was added, and incubation was continued for 24 h at 37 °C. Next, the ProteoStat reagent was added prior to the fluorescence measurement. Control conditions used phosphate buffer saline as a substitute for the antibodies. Other controls carried out included measurements with antibodies and arachidonic acid in the absence of tau and measurements without arachidonic acid or tau.

Enzyme-Linked Immunosorbent Assay (ELISA). For sandwich ELISA, tau protein at 11 μg mL^{-1} was coated on a 96-well Nunc Maxisorp plate overnight at 5 °C. The plate was washed three times with PBS (pH 7.2) containing 0.05% Tween-20 (PBS-T). Each antibody was diluted 4-fold in PBS-T with 1% bovine serum albumin (PBS-T-BSA) to 1.95, 7.81, 31.25, 125, and 500 ng mL^{-1} and placed into wells (100 μL each) overnight at 5 °C. The plate was then rinsed as described above. The plate was then treated with SuperBlock to reduce nonspecific binding of the secondary antibody. Next, the plate was incubated with biotinylated monoclonal antibody 6E10 (1:1000 dilution in PBS-T-BSA) for 1 h at 37 °C followed by streptavidin−alkaline phosphatase (1:1000 dilution in PBS-T) for 1 h at 37 °C. *p*-Nitrophenol phosphate (Sigma-Aldrich Co.; 5 mg in 40 mL of 1 M diethanolamine buffer (pH 9.8)) was added, and the optical density was read at 405 nm with a V_{max} kinetic microplate reader at 7.5 min or until the optical density reached a value of 1.0 for each antibody.

RESULTS AND DISCUSSION

The effects of antibodies specific to different regions of tau (N-terminus, MBD repeat sequences R1 and R4, and C-terminus) on tau aggregation and preformed tau aggregates were examined by transmission electron microscopy (TEM) and fluorescence spectroscopy to obtain a clearer understanding of how targeting different tau domains may influence tau aggregation. The IVIG product Gammagard, which is a mixture of antibodies, was also included in this study to determine its effects on tau aggregation and aggregation clearance. The binding affinities of the antibodies for tau were determined by ELISA.

Determination of Optimal Conditions for Arachidonic Acid-Induced Tau Aggregation. To induce tau protein aggregation, tau was mixed with arachidonic acid (ARA) under various conditions, and tau aggregation was evaluated by TEM. The results are shown in Figure 1. No oligomers, polymers, protofibrils, or fibrils were detected after a 24 h incubation of tau with ARA at 25 °C (final concentrations of tau and ARA: 95 μg mL^{-1} and 23 mg mL^{-1}, respectively) (Figure 1A). Increasing the final tau concentration to 250 μg mL^{-1} and the incubation temperature to 37 °C for 24 h produced predominantly small circular oligomers and polymers (Figure 1B). When the final tau and ARA concentrations were increased to 900 μg mL^{-1} and 30 mg mL^{-1}, respectively, with the temperature maintained at 37 °C, larger tau aggregates were observed after 24 h (Figure 1C).

Increasing the incubation time for the latter conditions to 48 h resulted in more extensive fibril formation (100−700 nm in length) as well as the formation of oligomers and polymers (Figure 1D). On the basis of these findings, the optimal aggregation formation protocol was determined to be 900 μg mL^{-1} tau in the presence of 30 mg mL^{-1} ARA at 37 °C for 48 h. The buffer used in these experiments was 50 mM MES (pH 6.8), 100 mM NaCl, and 0.5 mM EDTA, unless otherwise specified. The slightly acidic pH value was used to mimic the microenvironment that may be present in neurons. These

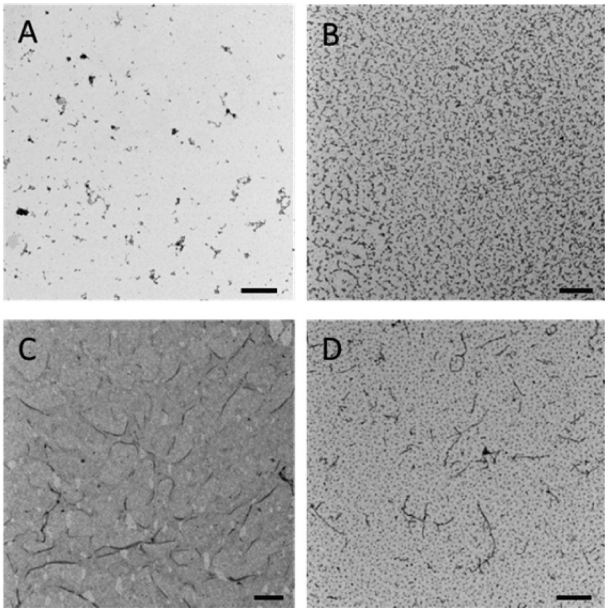

Figure 1. Tau aggregation under various conditions. (A) 95 μg mL^{-1} tau in buffer (10 mM HEPES (pH 7.6), 100 mM NaCl, 5 mM DTT, 0.1 mM EDTA (pH 6.8)) mixed with 23 mg mL^{-1} arachidonic acid (ARA) at 25 °C for 24 h (no fibrils are detected). In a buffer of 50 mM MES (pH 6.8), 100 mM NaCl, 0.5 mM EDTA: (B) 250 μg mL^{-1} tau mixed with 23 mg mL^{-1} ARA at 37 °C for 24 h (small circular oligomers and polymers are seen), (C) 900 μg mL^{-1} tau mixed with 30 mg mL^{-1} ARA for 37 °C at 24 h (small aggregates are formed), and (D) 900 μg mL^{-1} tau mixed with 30 mg mL^{-1} ARA at 37 °C for 48 h (more extensive fibrils are formed along with oligomers and polymers). Scale bar = 500 nm.

conditions were employed for subsequent studies to determine the effects of anti-tau antibodies and the IVIG on tau aggregation and preformed tau aggregates. Tau aggregation was monitored by fluorescence spectroscopy using the ProteoStat protein aggregation assay. The sensitivity of the ProteoStat assay is several orders of magnitude higher than that of the standard thioflavin T assay and has been used for the detection of α-synuclein aggregation,[28] intracellular amyloid-β structures,[29] amyloid fibrils, and tau in tissues.[30] The ProteoStat dye is a molecular rotor that has an absorption maximum of 500 nm and an emission maximum of 600 nm. Tau aggregation was monitored as a function of tau concentration and aggregation time. ProteoStat dye was added to determine the extent of β-sheet formation, commonly found during tau aggregation, by fluorescence spectroscopy. Tau concentration-dependent measurements were carried out by increasing the tau concentration during aggregation to 0, 1, 10, and 100 pg mL^{-1}, 1, 10, and 100 ng mL^{-1}, and 1, 10, 100, 200, 300, 400, 500, 600, 700, 800, 900, and 1000 μg mL^{-1}. In Figure 2A, saturation of the fluorescence intensity was observed above 800 μg mL^{-1} tau after 48 h of aggregation at 37 °C in the presence of 30 mg mL^{-1} ARA. The linear tau concentration range was detected to be between 400 and 800 μg mL^{-1}. Time-dependent aggregation was carried out with 900 μg mL^{-1} tau and 30 mg mL^{-1} ARA at 37 °C by stopping the aggregation at time intervals of 0, 3, 8, 10, 15, 30, and 60 min and 2, 3, 4, 6, 8, 12, 24, and 48 h. Figure 2B depicts the fluorescence intensity as a function of aggregation time. The fluorescence intensity reached saturation after only 30 min of aggregation. However,

DOI: 10.1021/bi501272x
Biochemistry 2015, 54, 293−302

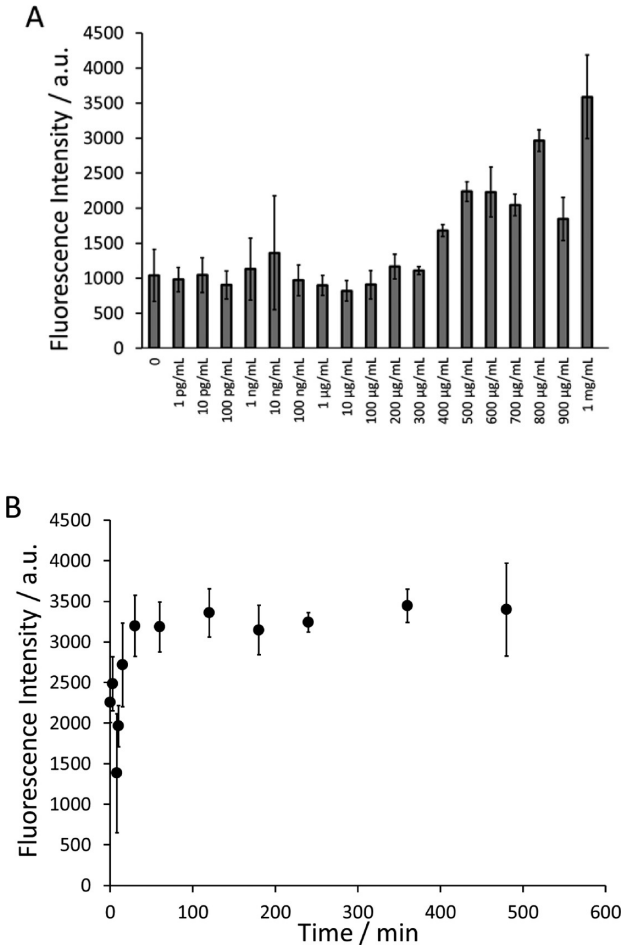

Figure 2. Fluorescence intensity during tau aggregation. Fluorescence intensity of (A) concentration-dependent tau aggregation ([ARA] = 30 mg mL^{-1}, incubation time = 48 h, incubation temperature = 37 °C) and (B) time-dependent tau aggregation under various conditions ([tau] = 900 μg mL^{-1}, [ARA] = 30 mg mL^{-1}, incubation temperature = 37 °C).

to visualize tau aggregates by TEM, a much longer aggregation time (48 h) was necessary.

Effects of Antibodies Targeting Various Regions of Tau on Tau Aggregation. Tau aggregation was performed as described above (900 μg mL^{-1} tau, 30 mg mL^{-1} ARA, 37 °C, 48 h) with the inclusion of anti-tau antibodies or PBS buffer at pH 6.8 as the negative control. Briefly, 10 μL of tau was combined with 0.5 μL of commercial anti-tau antibodies and 0.5 μL of arachidonic acid. The antibodies utilized were anti-tau 1−150 ("D-8"), anti-tau 259−266 ("Paired-262"), anti-tau 341−360 ("A-10"), and anti-tau 404−441 ("Tau-46"), which bind to tau's N-terminus, MBD repeat sequences R1 and R4, and C-terminus, respectively (Figure 3).

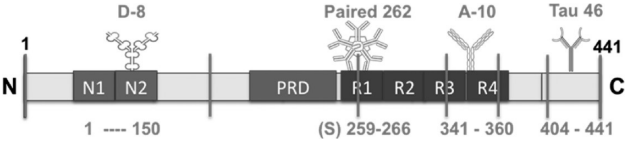

Figure 3. Schematic of the 441 isoform of tau targeted by the specific antibodies D-8, A-10, and Tau-46, which are monoclonal, and Paired-262, which is polyclonal.

The final concentrations of the A-10, D-8, Paired-262, and Tau-46 antibodies were each 9.1 μg mL^{-1}. Overall, the tau concentration was in great excess compared to the antibody concentration. The effects of the anti-tau antibodies on tau aggregation morphology are shown in Figure 4. Tau fibrils,

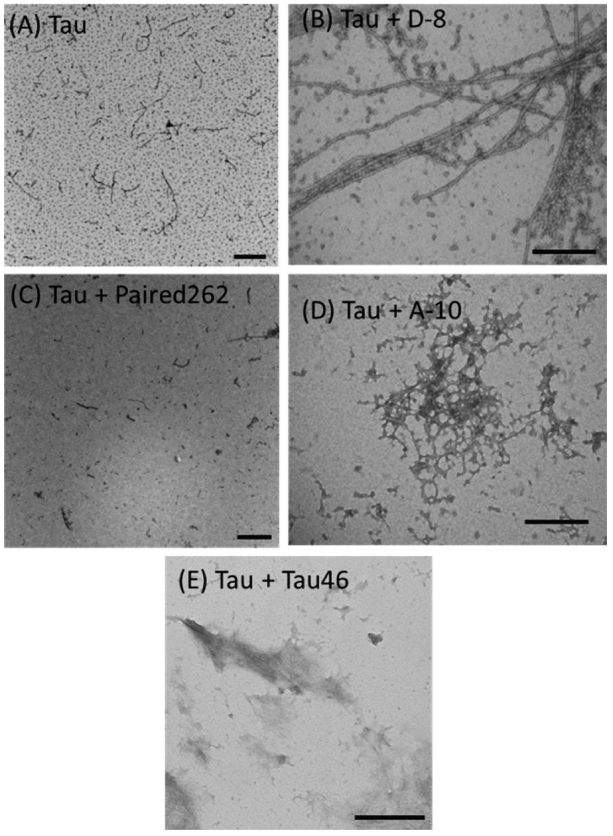

Figure 4. TEM images of tau aggregation in the absence and presence of anti-tau antibodies. (A) Tau fibrils, oligomers, and polymers were found when tau aggregation was performed in the absence of antibodies. (B) Tau oligomers, polymers, fibrils, and extensive fibrillar networks were found in the presence of antibody D-8. (C) The formation of tau fibrils was reduced in the presence of antibody Paired-262, although small protofibrils remained. (D) Tau protofibril and fibril formation was prevented in the presence of antibody A-10, although small oligomers, polymers, and amorphous aggregates were still present. (E) Extensive fibril formation and amorphous aggregates were found when antibody Tau-46 was included in the tau aggregation reaction. [Tau] = 900 μg mL^{-1}. [Antibodies] = 9 μg mL^{-1}. [ARA] = 30 mg mL^{-1}. Incubation time = 48 h. Incubation temperature = 37 °C. Scale bar = 500 nm.

oligomers, and polymers were observed as expected when the tau aggregation reaction was performed in the absence of antibodies (buffer control, Figure 4A). When the D-8 antibody (mouse anti-tau 1−150 targeting tau's N-terminus) was included in the aggregation reaction, long fibrils and extensive fibrillar networks were seen (Figure 4B). Tau fibril length appeared to be longer than when the aggregation reaction was performed in the absence of antibody. Inclusion of antibody Paired-262 (anti-tau 259−266 targeting an epitope in tau's MBD repeat sequence R1) in the tau aggregation reaction reduced tau fibril formation, though small protofibrils were still present (Figure 4C). When antibody A-10 (mouse anti-tau 341−360 targeting a sequence within tau's MBD repeat sequence R4) was included in the aggregation reaction, tau

DOI: 10.1021/bi501272x
Biochemistry 2015, 54, 293−302

protofibril and fibril formation was prevented, though small oligomers, polymers, and amorphous aggregates were detected (Figure 4D).

Inclusion of antibody Tau-46 in the tau aggregation reaction results in fibril formation as well as amorphous aggregates (Figure 4E). The TEM findings indicate that antibodies to specific regions of tau exert very different effects on tau aggregation. Antibody Paired-262, targeting MBD repeat sequence R1, appeared to have the most pronounced effect by inhibiting the formation of tau aggregates. Antibody A-10, specific to MBD repeat sequence R4, also prevented tau fibril development but resulted in the generation of amorphous aggregates. Our results for Paired-262's inhibition of tau aggregation are similar to those reported by Taniguchi et al.[25] using the antibody RTA-1, which was also specific to MBD repeat sequence R1.

Unlike the Paired-262 antibody, which targeted residues 259−266, the RTA-1 antibody targeted a longer amino acid sequence (259−274). That study also found inhibition of tau aggregation with an antibody targeting tau's MBD repeat sequence R2 (273−283).[25] The present study did not include an antibody specific to MBD repeat sequence 2, but it did include antibody A-10, which was specific for a sequence in MBD repeat sequence R4. The inhibitory effects of this antibody on tau aggregation were not as effective as those of the Paired-262 antibody. In contrast, antibodies D-8 and Tau-46, targeting sequences in tau's N- and C-termini, respectively, did not appear to reduce tau aggregate formation. The finding that antibody Tau-46 had no inhibitory effect on tau aggregation was also similar to results reported by Taniguchi et al. with their C-terminal anti-tau antibody RTA-C, which targeted the sequence 426−441, whereas Tau-46 in this study targeted a much longer sequence (404−441). However, Taniguchi et al. also concluded that any antibody to tau would have a partial inhibitory effect on aggregation and that this effect seemed to be independent of antibody binding to tau.[25] Our results with antibody D-8 (specific to the N-fragment), which appeared to increase tau fibril formation, do not support this conclusion.

The aggregation of tau was also monitored by fluorescence spectroscopy using the ProteoStat aggregation assay, which detects β-sheet formation during aggregation. Notably, this assay was carried out under conditions identical to those of TEM analysis by keeping the tau, antibodies, and ARA concentrations constant. Tau aggregation in the presence of various antibodies was measured after 48 h of aggregation at 37 °C. Figure 5 depicts the fluorescence intensities of monomeric tau prior to aggregation and aggregated tau. Notably, aggregated tau exhibited fluorescence intensity 3-fold higher than that of monomeric tau, evidence of β-sheet formation during aggregation. Tau aggregation was monitored by fluorescence spectroscopy in the presence of various antibodies as well. The plot of fluorescence intensity as a function of antibody type in Figure 5 indicates that, on average, tau aggregation in the presence of antibodies produced a signal similar to that of tau aggregated in the absence of antibodies. The fluorescence intensities in the presence of antibodies were in the 2500−3400 a.u. range. The similarity in fluorescence intensity in the absence and presence of antibodies may suggest that all tau aggregates contain some β-sheet structures even when aggregated in the presence of anti-tau antibodies. This possibility is supported by TEM images in Figure 4, which showed some evidence of tau aggregation even in the presence of the Paired-262 antibody. This aggregation translated into a relatively high fluorescence intensity using the extremely sensitive ProteoStat aggregation assay.

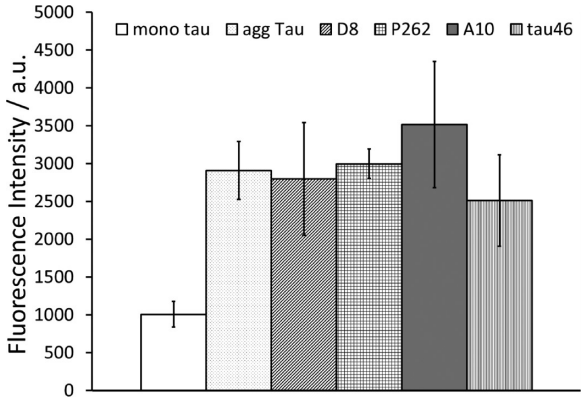

Figure 5. Plot of fluorescence intensity of tau as a function of antibodies during aggregation. Fluorescence intensity was measured for monomeric tau (mono tau) and aggregated tau (agg tau) in the absence of antibodies, as well as in the presence of D-8 (D8), Paired-262 (P262), A-10 (A10), and Tau-46 antibodies (tau46). [Tau] = 900 μg mL^{-1}. [ARA] = 30 mg mL^{-1}. 48 h incubation at 37 °C.

The high level of fluorescence in the presence of Paired-262 during aggregation may be explained by significant aggregation at the high protein concentration of 900 μg mL^{-1}. The ProteoStat protein aggregation assay is highly sensitive to aggregation of protein and can detect aggregation of IgG as low as a few percent with signal saturation occurring at 20% aggregation. The high β-sheet content in certain tau conformations may promote dye binding and result in the high fluorescence intensity. Hence, the nonfibrillar morphologies formed in the presence of Paired-262, A-10, and Tau-46 shown in Figure 4C−E, respectively, may contain a significant amount of β-sheet content, which in turn would generate a strong fluorescence signal.

Effects of Antibodies Targeting Various Regions of Tau on Preformed Tau Aggregates. Tau aggregates were generated as described above. Then, anti-tau antibodies were added, and incubation was continued for an additional 24 h at 37 °C. The results are shown in Figure 6.

The negative control (addition of buffer rather than one of the antibodies) resulted in long tau fibrils as expected (Figure 6A). When antibody D-8 was incubated with the preformed aggregates, fibrous strands were observed with minimal protofibrils at the periphery of the TEM grid (Figure 6B). Addition of antibody Paired-262 to preformed aggregates resulted in nearly complete degradation of the fibrils, although short protofibrils, oligomers, and polymers remained (Figure 6C). After incubation of preformed tau aggregates with antibody A-10, tau protofibrils, oligomers, and polymers were present, but tau fibrillar networks were missing (Figure 6D). Tau-46 antibody had little effect on preaggregated tau (Figure 6E). These findings indicated that the effects of the antibodies used in this study on tau aggregation appeared to correlate with their effects on preformed tau aggregates.

The antibodies targeting tau's MBD domains impaired tau aggregation and degraded preformed tau aggregates, whereas the antibodies targeting tau's N- and C-termini did not exert these effects. The tau morphologies generated in the presence of antibodies during tau aggregation and degradation varied with the different antibodies. These results suggest the possibility of distinct pathways during the aggregation and

DOI: 10.1021/bi501272x
Biochemistry 2015, 54, 293−302

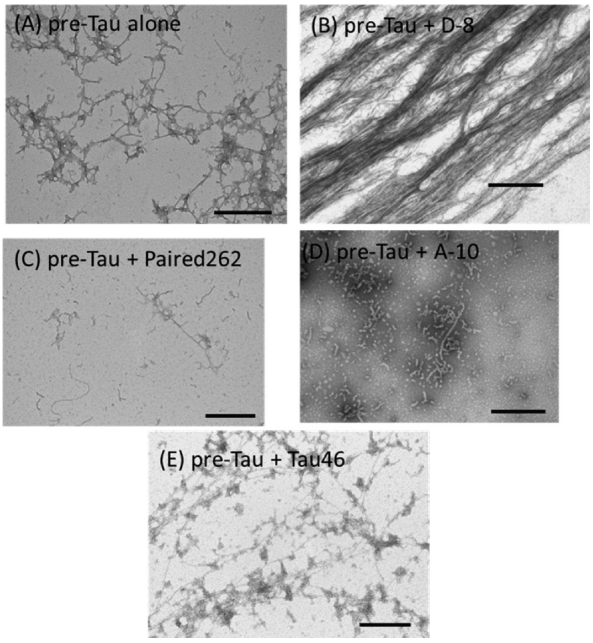

Figure 6. Effects of antibodies targeting various regions of tau on preformed tau aggregates. (A) Addition of buffer resulted in long tau fibrils as expected. (B) Addition of antibody D-8 produced long tau fibrils and fibrous strands. (C) Antibody Paired-262 degraded preformed tau fibrils, although short protofibrils, oligomers, and polymers remained. (D) Incubation of preformed tau aggregates with antibody A-10 resulted in tau protofibrils, oligomers, and polymers but no tau fibrils. (E) Tau-46 antibody had little effect on preaggregated tau. [Tau] = 900 μg mL^{-1}. [ARA] = 30 mg mL^{-1}. [Antibodies] = 9 μg mL^{-1}. Scale bar = 500 nm.

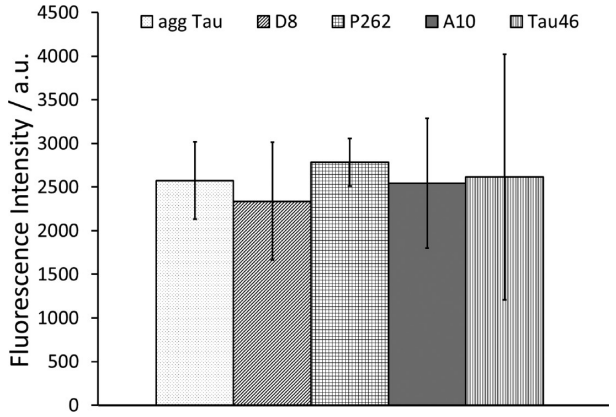

Figure 7. Plot of fluorescence intensity of tau as a function of antibodies during disaggregation. Fluorescence intensity was measured for aggregated tau (agg tau) in the absence and presence of antibodies D-8 (D8), Paired-262 (P262), A-10 (A10), and Tau-46 (tau46). [Tau] = 900 μg mL^{-1}. [ARA] = 30 mg mL^{-1}. [Antibodies] = 9 μg mL^{-1}. Tau aggregate generation during a 48 h incubation at 37 °C, followed by an additional 24 h incubation in the presence of antibodies.

degradation of tau; in other words, antibody-mediated degradation of tau may not simply be the reverse process of its aggregation. For example, antibody A-10, which targeted MBD repeat sequence R4, produced amorphous networks during tau aggregation (Figure 4D) but small oligomers, polymers, and short filaments during degradation (Figure 6D). In addition to the TEM analysis of the antibodies' effects on the degradation of preformed tau aggregates, their effects were also measured by fluorescence spectroscopy as shown in Figure 7.

The fluorescence intensity of preaggregated tau was similar in the absence and presence of antibodies. The data indicated that even in the presence of the most effective antibody (Paired-262 based on TEM findings), significant aggregation remained as indicated by high fluorescence intensity. High fluorescence intensities (>2000 a.u.) were observed for the partial fibrillar morphologies in Figure 6C and D in the presence of Paired-262 and A-10, respectively, indicating that a β-sheet structural motif is present. While TEM is a useful tool for characterizing the size and morphology of aggregates, even the smallest morphological features visible by TEM imaging may be based on a β-sheet structure. Conversely, fluorescence measurements are sensitive to the β-sheet structure in general, regardless of aggregate size or morphology. The negative control experiments for the fluorescence studies were performed with tau protein, ARA, and the respective negative control immunoglobulins for these antibodies (normal rabbit and mouse (MOPC-21) IgG). These normal immunoglobulins did not induce any change in fluorescence intensity when tau was aggregated or when they were used to treat preaggregated tau.

Effects of IVIG Gammagard and Normal Human IgG1 on Tau Aggregation and Preformed Tau Aggregates. The IVIG product Gammagard and normal human IgG1 (human myeloma protein) were included in the tau aggregation reaction and were incubated with preformed tau aggregates. Normal human IgG1 was used as a negative control for Gammagard. IVIG products differ from normal human IgG1 in that they are generated from pooled, purified plasma immunoglobulins (>95% IgG) from large numbers (typically ≥10000) of healthy donors. These products are used to treat many autoimmune, infectious, and idiopathic disorders. IVIG is thought to contain the complete range of antibodies in the human repertoire (estimated at 10^9).[31] Including Gammagard in the tau aggregation reaction appeared to reduce the extent of tau fibril formation compared to the extent of that including normal human IgG1, although oligomers, polymers, and protofibrils still developed (Figure 8A and B).

Fibril formation reduction with the IVIG was not as pronounced as with the Paired-262 antibody. Incubation of preformed tau aggregates with Gammagard appeared to reduce tau fibril formation (Figure 8C), whereas the inclusion of normal human IgG1 had little effect on preformed tau aggregates (Figure 8D). Our previous studies indicated that Gammagard and other IVIG products contain antibodies specific to recombinant human tau (tau 441)[32] that can bind specifically to tau's four MBD repeat sequences as well as to its N- and C-terminal sequences.[33] Gammagard's effects on tau aggregation and on preformed tau aggregates are therefore likely to be the result of its binding to multiple regions on tau. On the basis of our findings in the present study with commercial anti-tau antibodies, Gammagard's binding to some of these sites (MBD repeat sequences R1 and R4, for example) would have the potential for reducing tau aggregation, whereas its binding to tau's N- and C-termini could have the opposite effect. Whether other IVIG products possess the partial inhibitory effects on tau aggregation that was observed for Gammagard is unknown.

The effect of the IVIG and normal human IgG1 on tau aggregation and disaggregation was also monitored by fluorescence spectroscopy. Figure 9 shows the fluorescence intensity of tau aggregation or disaggregation in the presence of

DOI: 10.1021/bi501272x
Biochemistry 2015, 54, 293−302

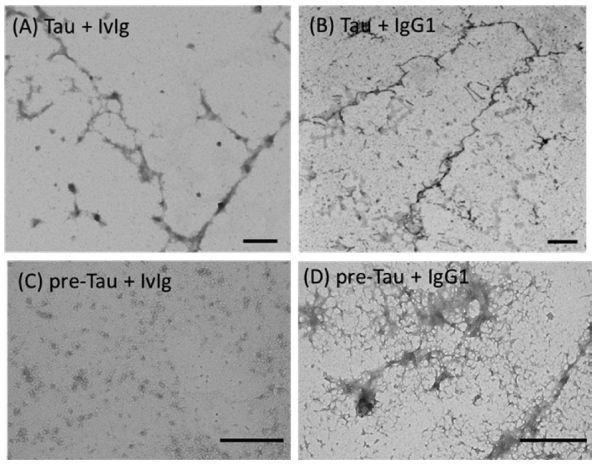

Figure 8. Effects of IVIG Gammagard and normal human IgG1 on tau aggregation and preformed tau aggregates. (A) Inclusion of the IVIG product Gammagard in the tau aggregation reaction reduced the extent of tau fibril formation compared to those seen upon inclusion of (B) normal human IgG1 (human myeloma proteins), although oligomers, polymers, and protofibrils still developed. (C) Addition of IVIG product Gammagard to preformed tau aggregates reduced tau fibril length. (D) Addition of normal human IgG1 produced fibrils and amorphous aggregates. Preformed tau aggregates were incubated at 37 °C for 24 h with normal human IVIG (C) or IgG1 (D). [Tau] = 900 μg mL^{-1}. [ARA] = 30 mg mL^{-1}. [Antibodies] = 45 μg mL^{-1}. Scale bar = 500 nm.

IVIG or IgG1. During tau aggregation, the addition of IVIG significantly increased the fluorescence intensity from 2800 to 4600 a.u. The fluorescence increase may be due to dye binding to the IVIG formulation, which contains immunoglobulin aggregates. However, the control condition with the IVIG in the absence of tau did not produce high fluorescence (results not shown).

Inclusion of normal human IgG1 during aggregation produced a slight decrease in fluorescence intensity compared to that of tau aggregation in the absence of antibodies. When the IVIG and IgG1 were added during the tau disaggregation study, fluorescence intensities similar to that of preaggregated tau further incubated in the absence of antibodies were observed.

Antibody Binding Affinity for Tau. To determine the binding affinity of each antibody, ELISAs were performed. Briefly, tau protein was coated on ELISA plates at 11 μg mL^{-1}, and then the plates were incubated with antibodies at concentrations of 0, 1.95, 7.81, 21.25, 125, and 500 ng mL^{-1}. This was followed by incubation with a biotinylated monoclonal antibody (6E10), streptavidin−alkaline phosphatase conjugate, and *p*-nitrophenol phosphate substrate as previously reported.[34] 6E10 is a commonly used mouse monoclonal antibody specific to epitopes 3−8 of human amyloid beta.[35] The optical density (OD) was measured at 7.5 min, and OD values were plotted for all antibodies as a function of antibody concentration as shown in Figure 10. The order of increasing OD values was as follows: normal human IgG1 < A-10 < D-8 < Paired-262 < IVIG ≈ Tau-46. The OD_{405} values for normal IgG1, A-10, D-8, Paired-262, IVIG, and Tau-46 were 0.048, 0.086, 0.355, 0.800, 0.970, and 1.044, respectively. Hence, higher binding affinities were observed for Tau-46 and the IVIG, whereas normal human IgG1 and A-10 exhibited lower binding affinities. Because ELISA requires surface

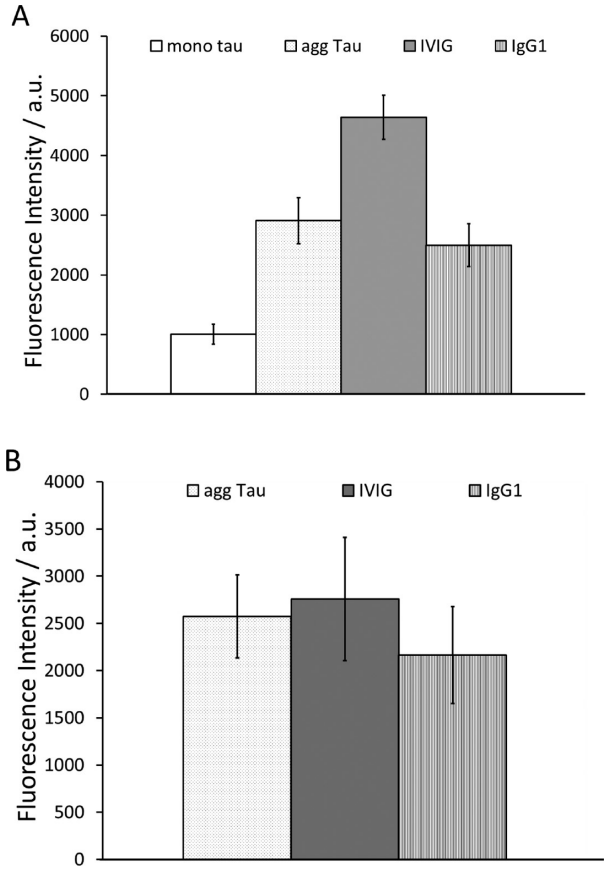

Figure 9. Plot of fluorescence intensity of tau as a function of IVIG or IgG1 antibodies during (A) aggregation and (B) disaggregation. (A) Fluorescence intensity was measured for monomeric tau (mono tau) and aggregated tau (agg tau) in the absence of antibodies. Tau aggregation was also carried out in the presence of the IVIG or IgG1 antibodies. [Tau] = 900 μg mL^{-1}. [ARA] = 30 mg mL^{-1}. [Antibodies] = 45 μg mL^{-1}. Incubation for 48 h at 37 °C. (B) Fluorescence intensity for aggregated tau (agg Tau) in the absence of antibodies. After tau aggregate formation, IVIG or IgG1 antibodies were added, and aggregation was continued for an additional 24 h at 37 °C. [Antibodies] = 45 μg mL^{-1}.

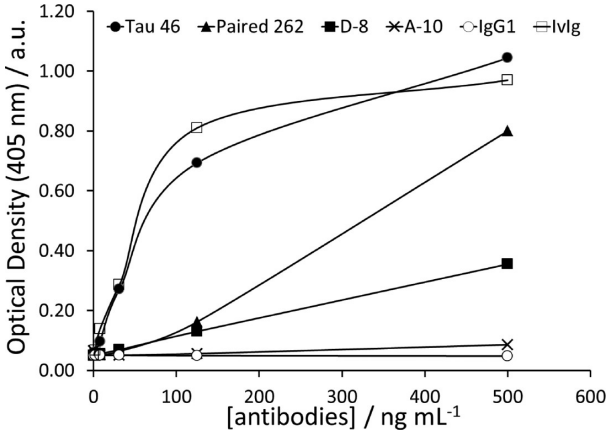

Figure 10. Plot of optical density for ELISA as a function of antibody concentration. Optical density was measured at 405 nm for binding of various antibodies at 0, 1.95, 7.81, 31.25, 125, and 500 ng mL^{-1} to tau protein. [Tau] = 11 μg mL^{-1}. Development time = 7.5 min.

immobilization of the tau protein, measurements on the binding affinity of an anti-tau antibody may also be affected by

DOI: 10.1021/bi501272x
Biochemistry 2015, 54, 293−302

the accessibility of the tau epitope(s) to which it binds. Nonspecific binding of each antibody was evaluated by coating the ELISA plate with bovine serum albumin (BSA) instead of tau and performing identical measurements. The OD_{405} values for binding of the anti-tau antibodies to BSA were at ~0.05, irrespective of their concentrations, which is similar to the OD_{405} value for the binding of normal human IgG1 to the tau protein. Notably, the OD_{405} values for IVIG binding to BSA increased with increasing IVIG concentration, with a maximum OD_{405} of 0.48. These findings indicate that the IVIG binds nonspecifically to BSA with a binding affinity lower than that for the tau protein (OD_{405} = 0.97).

The ELISA binding affinity data do not explain the marked effects of the antibodies targeting tau's MBD upon tau aggregation and on disaggregation of preformed tau aggregates. Hence, the extent of the antibody−antigen binding affinity does not appear to be related to the antibodies' effects on the aggregation of tau, unlike the role of the specific tau domains in the aggregation process. The possible reason for antibody affinity having a weaker effect on aggregation of tau than tau domains may be that a specific epitope within tau's MBD may not be critical for the aggregation process. Hence, the antibody affinity for the epitope within that sequence has little effect on tau aggregation. For example, A-10, which targets tau 341−360 sequence in MBD domain R4, exhibits one of the lowest binding affinities for tau protein (Figure 10) but dramatically reduces tau fibril formation (Figure 4D). It is unclear whether aggregation of tau via its repeat R domains in the MBD may interfere with antibody binding to these domains; if so, it would presumably decrease antibody binding affinity for these regions. The mechanisms by which antibody binding to tau's MBDs may result in inhibition of its aggregation and degradation of preformed tau aggregates are unclear.

Soluble tau is a natively unfolded protein[36] because of its low hydrophobic content.[37] Its misfolding can lead to pathological conformations; in particular, conformational changes that expose hydrophobic areas on tau monomers may promote their aggregation.[38] Tau's MBDs are critical for its aggregation;[22] thus, antibody binding to MBDs could inhibit the conformational changes required for tau aggregation. For example, chaperones function to maintain proteins in their properly folded state.[36] Anti-tau antibodies have been suggested to exert chaperone-like activity against pathological tau conformations,[39,40] preventing tau aggregation and/or degrading preformed tau aggregates. Whether such chaperone-like activity requires specific antibody binding to tau is unclear; however, Taniguchi et al.[25] suggested that because the F_c portion of an antibody is extremely hydrophobic, it may inhibit tau aggregation by disturbing hydrophobic interactions in the MBD. It would be informative to generate F_{ab} fragments from the antibodies used in the present study targeting the MBD (antibodies Paired-262 and A-10), and then determine whether the inhibitory effects of these antibodies on tau aggregates could be replicated by their F_{ab} fragments.

CONCLUSIONS

An antibody bound to tau's MBD repeat sequence R1 markedly inhibited ARA-mediated aggregation of tau and degraded preformed tau aggregates, and an antibody to tau's MBD repeat sequence R4 exerted similar but less pronounced effects. In contrast, antibodies specific for tau's N- and C-terminal regions did not reduce tau aggregates. Different tau morphologies were formed in the presence of these different antibodies, but they were mostly composed of a β-sheet structure. The tau species observed by TEM during aggregation in the presence of these antibodies were not necessarily the same as those seen after preformed tau aggregates were incubated with the antibodies. This result suggested that tau aggregation and degradation of tau aggregates in the presence of antibodies may not simply be reverse processes of each other (i.e., they may occur via different pathways). The IVIG product Gammagard partially inhibited tau aggregation and somewhat degraded preformed tau aggregates. The antibodies' effects on tau were related to antibody targeting to tau domains, but not to antibody−antigen binding affinities. These findings confirm that antibodies that target tau's MBDs may be useful for reducing tau pathology in AD and other tauopathies. For this reason, future cell culture studies will be carried out to determine the toxicity levels of each tau/antibody formulation on cells.

ASSOCIATED CONTENT

Supporting Information

TEM images and fluorescence spectroscopy data. This material is available free of charge via the Internet at http://pubs.acs.org.

AUTHOR INFORMATION

Corresponding Author

*E-mail: martic@oakland.edu. Tel: 1-248-370-3088.

Funding

This study was supported by an Oakland University−Beaumont Multidisciplinary Research Award to S.M. and D.A.L. Additional support for D.A.L. was provided by a donation from the Erb family.

Notes

The authors declare no competing financial interest.

ACKNOWLEDGMENTS

We thank Loan Dang (Eye Research Institute, Oakland University) and Alicia Withrow (Center for Advanced Microscopy, Michigan State University) for assistance with the TEM studies and Lynnae Smith and Andrea Klaver for their assistance with the ELISA studies.

ABBREVIATIONS

AD, Alzheimer's disease; MBD, microtubule binding domain; TEM, transmission electron microscopy

REFERENCES

(1) Weingarten, M. D., Lockwood, A. H., Hwo, S. Y., and Kirschener, M. W. (1975) A protein factor essential for microtubule assembly. *Proc. Natl. Acad. Sci. U.S.A. 72*, 1858−1862.

(2) Jaworski, T., Kügler, S., and Van Leuven, F. (2010) Modeling of tau-mediated synaptic and neuronal degeneration in Alzheimer's disease. *Int. J. Alzheimer's Dis. 2010* (2010), 573138-1−573138-10.

(3) Patterson, K. R., Remmers, C., Fu, Y., Brooker, S., Kanaan, N. M., Vana, L., Ward, S., Reyes, J. F., Philibert, K., Glucksman, M. J., and Binder, L. I. (2011) Characterization of prefibrillar Tau oligomers in vitro and in Alzheimer disease. *J. Biol. Chem. 286*, 23063−23076.

(4) Lublin, A. L., and Gandy, S. (2010) Amyloid-β oligomers: possible roles as key neurotoxins in Alzheimer's disease. *Mt. Sinai J. Med. 77*, 43−49.

(5) Clavaguera, F., Bolmont, T., Crowther, R. A., Abramowski, D., Frank, S., Probst, A., Fraser, G., Stalder, A. K., Beibel, M., Staufenbiel, M., Jucker, M., Goedert, M., and Tolnay, M. (2009) Transmission and spreading of tauopathy in transgenic mouse brain. *Nat. Cell Biol. 11*, 909−913.

DOI: 10.1021/bi501272x
Biochemistry 2015, 54, 293−302

(6) Kfoury, N., Holmes, B. B., Jiang, H., Holtzman, D. M., and Diamond, M. I. (2012) Trans-cellular propagation of Tau aggregation by fibrillar species. *J. Biol. Chem. 287*, 19440−19451.
(7) Aisen, P. S. (2008) Tarenflurbil: a shot on goal. *Lancet Neurol. 7*, 468−469.
(8) Holmes, C., Boche, D., Wilkinson, D., Yadegarfar, G., Hopkins, V., Bayer, A., Jones, R. W., Bullock, R., Love, S., Neal, J. W., Zotova, E., and Nicoll, J. A. (2008) Long-term effects of $A\beta_{42}$ immunisation in Alzheimer's disease: follow-up of a randomised, placebo-controlled phase I trial. *Lancet 372*, 216−223.
(9) St George-Hyslop, P. H., and Morris, J. C. (2008) Will anti-amyloid therapies work for Alzheimer's disease? *Lancet 372*, 180−182.
(10) Asuni, A. A., Boutajangout, A., Quartermain, D., and Sigurdsson, E. M. (2007) Immunotherapy targeting pathological tau conformers in a tangle mouse model reduces brain pathology with associated functional improvements. *J. Neurosci. 27*, 9115−9129.
(11) Boutajangout, A., Quartermain, D., and Sigurdsson, E. M. (2010) Immunotherapy targeting pathological tau prevents cognitive decline in a new tangle mouse model. *J. Neurosci. 30*, 16559−16566.
(12) Boimel, M., Grigoriadis, N., Lourbopoulos, A., Haber, E., Abramsky, O., and Rosenmann, H. (2010) Efficacy and safety of immunization with phosphorylated tau against neurofibrillary tangles in mice. *Exp. Neurol. 224*, 472−485.
(13) Bi, M., Ittner, A., Ke, Y. D., Götz, J., and Ittner, L. M. (2011) Tau-targeted immunization impedes progression of neurofibrillary histopathology in aged P301L tau transgenic mice. *PLoS One 6*, e26860.
(14) Troquier, L., Caillierez, R., Burnouf, S., Fernandez-Gomez, F. J., Grosjean, M. E., Zommer, N., Sergeant, N., Schraen-Maschke, S., Blum, D., and Buee, L. (2012) Targeting phospho-Ser422 by active Tau Immunotherapy in the THYTau22 mouse model: a suitable therapeutic approach. *Curr. Alzheimer Res. 9*, 397−405.
(15) Theunis, C., Crespo-Biel, N., Gafner, V., Pihlgren, M., López-Deber, M. P., Reis, P., Hickman, D. T., Adolfsson, O., Chuard, N., Ndao, D. M., Borghgraef, P., Devijver, H., Van Leuven, F., Pfeifer, A., and Muhs, A. (2013) Efficacy and safety of a liposome-based vaccine against protein Tau, assessed in tau.P301L mice that model tauopathy. *PLoS One 8*, e723.
(16) Sigurdsson, E. M. (2008) Immunotherapy targeting pathological tau protein in Alzheimer's disease and related tauopathies. *J. Alzheimer's Dis. 15*, 157−168.
(17) Chai, X., Wu, S., Murray, T. K., Kinley, R., Cella, C. V., Sims, H., Buckner, N., Hanmer, J., Davies, P., O'Neill, M. J., Hutton, M. L., and Citron, M. (2011) Passive immunization with anti-Tau antibodies in two transgenic models: reduction of Tau pathology and delay of disease progression. *J. Biol. Chem. 286*, 34457−34467.
(18) Boutajangout, A., Ingadottir, J., Davies, P., and Sigurdsson, E. M. (2011) Passive immunization targeting pathological phospho-tau protein in a mouse model reduces functional decline and clears tau aggregates from the brain. *J. Neurochem. 118*, 658−667.
(19) St-Amour, I., Paré, I., Tremblay, C., Coulombe, K., Bazin, R., and Calon, F. (2014) IVIg protects the 3xTg-AD mouse model of Alzheimer's disease from memory deficit and $A\beta$ pathology. *J. Neuroinflammation 11*, 54−69.
(20) Congdon, E. E., Gu, J., Sait, H. B., and Sigurdsson, E. M. (2013) Antibody uptake into neurons occurs primarily via clathrin-dependent Fcγ receptor endocytosis and is a prerequisite for acute tau protein clearance. *J. Biol. Chem. 288*, 35452−35465.
(21) Goode, B. L., Chau, M., Denis, P. E., and Feinstein, S. C. (2000) Structural and functional differences between 3-repeat and 4-repeat tau isoforms. Implications for normal tau function and the onset of neurodegenerative disease. *J. Biol. Chem. 275*, 38182−38189.
(22) von Bergen, M., Friedhoff, P., Biernat, J., Heberle, J., Mandelkow, E.-M., and Mandelkow, E. (2000) Assembly of τ protein into Alzheimer paired helical filaments depends on a local sequence motif (^{306}VQIVYK^{311}) forming β structure. *Proc. Natl. Acad. Sci. U.S.A. 97*, 5129−5134.
(23) Tomoo, K., Yao, T. M., Minoura, K., Hiraoka, S., Sumida, M., Taniguchi, T., and Ishida, T. (2005) Possible role of each repeat structure of the microtubule-binding domain of the tau protein in in vitro aggregation. *J. Biochem. 138*, 413−423.
(24) Combs, B., and Gamblin, T. C. (2012) FTDP-17 Tau mutations induce distinct effects on aggregation and microtubule interactions. *Biochemistry 51*, 8597−8607.
(25) Taniguchi, T., Sumida, M., Hiraoka, S., Tomoo, K., Kakehi, T., Minoura, K., Sugiyama, S., Inaka, K., Ishida, T., Saito, N., and Tanaka, C. (2005) Effects of different anti-tau antibodies on tau fibrillogenesis: RTA-1 and RTA-2 counteract tau aggregation. *FEBS Lett. 579*, 1399−1404.
(26) Yanamandra, K., Kfoury, N., Jiang, H., Mahan, T. E., Ma, S., Maloney, S. E., Wozniak, D. F., Diamond, M. I., and Holtzman, D. M. (2013) Anti-tau antibodies that block tau aggregate seeding in vitro markedly decrease pathology and improve cognition in vivo. *Neuron 80*, 402−414.
(27) Castillo-Carranza, D. L., Sengupta, U., Guerrero-Muñoz, M. J., Lasagna-Reeves, C. A., Gerson, J. E., Singh, G., Estes, D. M., Barrett, A. D., Dineley, K. T., Jackson, G. R., and Kayed, R. (2014) Passive immunization with tau oligomer monoclonal antibody reverses tauopathy phenotypes without affecting hyperphosphorylated neurofibrillary tangles. *J. Neurosci. 34*, 4260−4272.
(28) Watanabe, Y., Tatebe, H., Taguchi, K., Endo, Y., Tokuda, T., Mizuno, T., Nakagawa, M., and Tanaka, M. (2012) p62/SQSTM1-dependent autophagy of Lewy body-like α-synuclein inclusions. *PLoS One 7*, e52868.
(29) Chakrabortee, S., Liu, Y., Zhang, L., Matthews, H. R., Zhang, H., Pan, N., Cheng, C. R., Guan, S. H., Guo, D. A., Huang, Z., Zheng, Y., and Tunnacliffe, A. (2012) Macromolecular and small-molecule modulation of intracellular $A\beta_{42}$ aggregation and associated toxicity. *Biochem. J. 442*, 507−515.
(30) Shen, D., Coleman, J., Chan, E., Nicholson, T. P., Dai, L., Sheppard, P. W., and Patton, W. F. (2011) Novel cell- and tissue-based assay for detectiong misfolded and aggregated protein accumulation within aggresomes and inclusion bodies. *Cell Biochem. Biophys. 60*, 173−185.
(31) Bayry, J., Kazatchkine, M. D., and Kaveri, S. V. (2007) Shortage of human intravenous immunoglobulin—reasons and possible solutions. *Nat. Clin. Pract. Neurol. 3*, 120−121.
(32) Smith, L. M., Coffey, M. P., Klaver, A. C., and Loeffler, D. A. (2013) Intravenous immunoglobulin products contain specific antibodies to recombinant human tau protein. *Int. Immunopharmacol. 16*, 424−428.
(33) Smith, L. M., Coffey, M. P., and Loeffler, D. A. (2014) Specific binding of intravenous immunoglobulin products to tau peptide fragment. *Int. Immunopharmacol. 21*, 279−282.
(34) Klaver, A. C., Patrias, L. M., Finke, J. M., and Loeffler, D. A. (2011) Specificity and sensitivity of the $A\beta$ oligomer ELISA. *J. Neurosci. Methods 195*, 249−254.
(35) Youmans, K. L., Tai, L. M., Kanekiyo, T., Stine, W. B., Jr., Michon, S. C., Nwabuisi-Heath, E., Manelli, A. M., Fu, Y., Riordan, S., Eimer, W. A., Binder, L., Bu, G., Yu, C., Hartley, D. M., and LaDu, M. J. (2012) Intraneuronal $A\beta$ detection in 5xFAD mice by a new $A\beta$-specific antibody. *Mol. Neurodegener. 7*, 8−22.
(36) Pickhardt, M., Gazova, Z., von Bergen, M., Khlistunova, I., Wang, Y., Hascher, A., Mandelkow, E. M., Biernat, J., and Mandelkow, E. (2005) Anthraquinones inhibit tau aggregation and dissolve Alzheimer's paired helical filaments in vitro and in cells. *J. Biol. Chem. 280*, 3628−3635.
(37) Davidowitz, E. J., Chatterjee, I., and Moe, J. G. (2008) Targeting tau oligomers for therapeutic development for Alzheimer's disease and tauopathies. *Curr. Top. Biotechnol. 4*, 47−64.
(38) Voss, K., Combs, B., Patterson, K. R., Binder, L. I., and Gamblin, T. C. (2012) Hsp70 alters tau function and aggregation in an isoform specific manner. *Biochemistry 51*, 888−898.
(39) Zilka, M., Kontsekova, E., and Novak, M. (2008) Chaperone-like antibodies targeting misfolded tau protein: new vistas in the immunotherapy of neurodegenerative foldopathies. *J. Alzheimer's Dis. 15*, 169−179.

DOI: 10.1021/bi501272x
Biochemistry 2015, 54, 293−302

(40) Kontsekova, E., Ivanovova, N., Handzusova, M., and Novak, M. (2009) Chaperone-like antibodies in neurodegenerative tauopathies: implication for immunotherapy. *Cell. Mol. Neurobiol. 29*, 793−798.

DOI: 10.1021/bi501272x
Biochemistry 2015, 54, 293−302